Production d'énergie (hydraulique, thermique et nucléaire)

CALCUL PAR SYNTHESE MODALE DES MODES COUPLES FLEXION DES AUBAGES/TORSION DE L'ARBRE D'UN GROUPE TURBO-ALTERNATEUR

MODAL ANALYSIS OF BLADE BENDING AND TORSIONAL SHAFT COUPLING BY COMPONENT MODE SYNTHESIS

96NB00098

Direction des Etudes et Recherches

EDF
Electricité de France

Direction des Etudes et Recherches

SERVICE ENSEMBLES DE PRODUCTION
Département Acoustique et Mécanique Vibratoire

Octobre 1995

VARE C.

CALCUL PAR SYNTHESE MODALE DES MODES COUPLES FLEXION DES AUBAGES/TORSION DE L'ARBRE D'UN GROUPE TURBO-ALTERNATEUR

MODAL ANALYSIS OF BLADE BENDING AND TORSIONAL SHAFT COUPLING BY COMPONENT MODE SYNTHESIS

Pages : 13

96NB00098

Diffusion : J.-M. Lecœuvre
EDF-DER
Service IPN. Département SID
1, avenue du Général-de-Gaulle
92141 Clamart Cedex

ISSN 1161-0611

SYNTHÈSE :

Le département Acoustique et Mécanique Vibratoire de la Direction des Etudes et Recherches d'EDF est chargé d'effectuer des calculs par éléments finis destinés à l'étude du comportement vibratoire des composants des centrales nucléaires. En raison de la dimension et de la complexité géométrique de certains de ces composants, EDF a mis au point des méthodes de synthèse modale permettant l'analyse vibratoire des structures les plus importantes. On a ainsi implanté les méthodes de Craig-Bampton et de Mac Neal dans le code de mécanique générale d'EDF : le Code_Aster.

La méthode de synthèse modale de Craig-Bampton a été utilisée pour étudier le couplage entre la flexion des ailettes et la torsion de l'arbre d'un groupe turbo-alternateur. Quatre sous-structures ont été définies pour effectuer ce calcul : un alternateur, un rotor basse pression, un rotor haute pression et une ailette.

Les résultats des calculs modaux montrent une bonne corrélation avec les mesures expérimentales (erreur < 2,5 %). De surcroît, on constate que le calcul par synthèse modale est sept fois plus rapide que le calcul direct, et que la différence entre les deux méthodes est très faible (erreur < 1 %), ce qui démontre la précision des méthodes de sous-structuration dynamique.

EXECUTIVE SUMMARY :

The Acoustics and Vibration Mechanics Branch of E.D.F.'s Research and Development Division is in charge of performing finite element calculations, for the study of the vibratory behaviour of nuclear components. Due to the size and the geometrical complexity of some of these components, E.D.F. has developed sub-structure synthesis methods for modal analysis of large structures. Both Craig-Bampton's and Mac Neal's methods have been implemented in the general mechanics code of E.D.F. : the Aster_Code.

Craig-Bampton sub-structure synthesis approach was used to study the coupling between blade bending and torsional shaft of a turbine generator set. Four sub-structures were defined to make the calculation : a generator, a low pressure rotor, a high pressure rotor and a blade.

The results of the modal calculation, show good agreement with the experimental measurements (error < 2,5 %). Moreover, we find that component mode synthesis is seven times faster than direct calculation and that the difference between the two methods is very slight (error < 1 %). It shows the accuracy of component mode synthesis methods.

MODAL ANALYSIS OF BLADE BENDING AND TORSIONAL SHAFT COUPLING BY COMPONENT MODE SYNTHESIS

C. VARE
Département Acoustique et Mécanique Vibratoire, EDF, Clamart, FRANCE

1 Introduction

The Acoustics and Vibration Mechanics Branch of E.D.F. 's Research and Development Division is in charge of performing finite element calculations, to ensure, by the design stage, the correct sizing of nuclear components submitted to vibratory loads. Due to the size and the geometrical complexity of some of these components, such analyses may lead to models whose number of degrees of freedom is large to the extent that computational processing is impraticable or too expensive. In order to limit the computer time and storage, E.D.F. has developed sub-structure synthesis methods for modal analysis of large structures. Both Craig-Bampton and

Mac Neal's methods have been implemented in the general mechanics code of E.D.F. : the *Aster Code*. [1].

Sub-structure synthesis methods consist in using simultaneously dynamic sub-structuring and modal superposition. The displacement of a sub-structure in the whole movement, thus results from interface forces which relate it to the other components. Moreover, each sub-structure is represented by a finite set of suitable admissible functions (Ritz 's transformation) which defines its projection base.

In this paper, we first present the eigen modes calculation method by component mode synthesis which was used for the industrial study : the Craig-Bampton method.

Then, the modal calculation of a turbine generator set whose bladings bending is coupled with the torsional shaft is shown. The comparisons with the experimental results and direct calculations are studied.

1.1 Notations

ω : pulsation (rad.s^{-1}),
$\mathbf{M}$: mass matrix from the finite element model,
$\mathbf{K}$: stiffness matrix from the finite element model,
$\mathbf{q}$: displacement vector from the finite element model,
$\mathbf{f}_L$: force vector at the interface of two sub-structures,
Φ : matrix of the sub-structure projection base,
η : generalized displacement vector,
$\mathbf{B}$: extraction matrix of the interface degrees of freedom.

The superscript k denotes the variables from sub-structure S^k. Moreover, the generalized variables are overlined. For example, $\overline{\mathbf{M}}^k$ is the generalized mass matrix from sub-structure S^k.

2 Component mode synthesis by Craig-Bampton method

Sub-structure synthesis methods consist in using simultaneously dynamic sub-structuring and modal superposition. Thus, each sub-structure is represented by a finite set of suitable admissible functions (Ritz 's transformation) which defines its projection base.

Both Craig-Bampton and Mac Neal's methods are implemented in the *Aster Code*. They can be distinguished by the use of different bases for the sub-structures.

On the one hand, Craig-Bampton uses, as projection base for the sub-structures, constrained modes and eigen modes with fixed interfaces [2]. On the other hand, Mac Neal uses, as projection base of the sub-structures, attachment modes and eigen modes with free interfaces [3].

In this paper, we present the Craig-Bampton method which was used for the modal calculation of the turbine generator set.

Let us consider an embedded-free beam, cut at its middle in 2 sub-structures (fig. 1) :

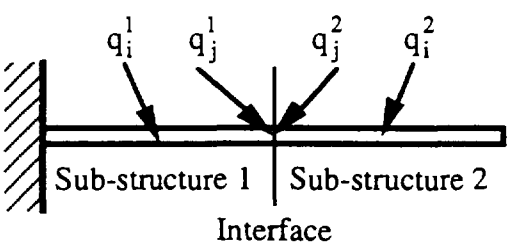

Fig. 1 : embedded-free beam

The subscript i (resp. j) denotes the inner (resp. interface) degrees of freedom. Then the displacement vector of the sub-structure S^k can be written :

$$\mathbf{q}^k = \begin{Bmatrix} \mathbf{q}_i^k \\ \mathbf{q}_j^k \end{Bmatrix} \quad (1)$$

The eigen modes of the projection base of Craig-Bampton method are obtained by fixing the interfaces :

Fig. 2 : eigen modes of the projection base of Craig-Bampton

They are obtained by solving the equation (2) :

$$\begin{matrix} \left(\mathbf{K}^k - \omega^2 \mathbf{M}^k\right)\mathbf{q}^k = 0 \\ \mathbf{q}_j^k = 0 \end{matrix} \quad (2)$$

Moreover, the constrained modes are obtained by applying an unit displacement to each interface degree of freedom, the others being fixed :

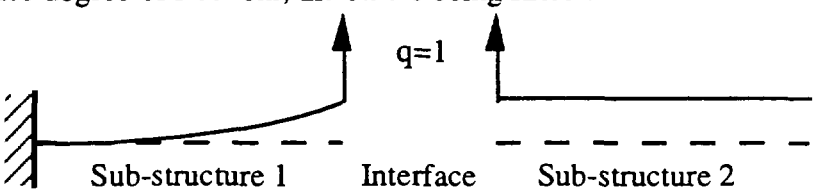

Fig. 3 : constrained modes of the projection base of Craig-Bampton

They are obtained by solving the equation (3) :

$$\begin{matrix} \mathbf{K}^k \mathbf{q}^k = F_j^k \\ \mathbf{q}_j^k = 1 \end{matrix} \quad (3)$$

These static modes are joined to the eigen modes of the sub-structures to reduce the truncation errors. In particular, it is obvious that without the contrained modes, the movement of interfaces would be impossible.

2.1 Dynamic equations verified by each sub-structure

Let us consider the finite element model of a sub-structure denoted S^k. The displacement of the sub-structure in the whole movement results from interface forces which relate it to the other components. So, the eigen value problem, applied to S^k can be written as following :

$$\left(\mathbf{K}^k - \omega^2 \mathbf{M}^k\right)\mathbf{q}^k = \sum_l \mathbf{f}^k_{L_{S^k \cap S^l}} \quad (4)$$

where : $\mathbf{K}^k$ is the stiffness matrix from the finite element model of S^k,

$\mathbf{M}^k$ is the mass matrix from the finite element model of S^k,

$\mathbf{f}^k_{L_{S^k \cap S^l}}$ is the interface force vector applied by S^l to S^k,

$\mathbf{q}^k$ is the displacement vector from the finite element model of S^k.

Let $\mathbf{B}_l^k$ be the extraction matrix of the degrees of freedom of S^k belonging to the $S^k \cap S^l$ interface. With this notation, equation (4) can be rewritten :

$$\left(\mathbf{K}^k - \omega^2 \mathbf{M}^k\right)\mathbf{q}^k = \sum_l \mathbf{B}_l^{kT} \mathbf{f}_L^k \quad (5)$$

where : $\mathbf{f}_L^k$ is the interface force vector applied to S^k.

The sub-structure is represented by a finite set of eigen modes and constrained modes which defines its projection base :

$$\Phi^k = \left(\varphi^k, \psi^k\right) \quad (6)$$

where : Φ^k is the projection base matrix of S^k,

φ^k is the eigen modes vector of S^k,

ψ^k is the constrained modes vector of S^k.

The displacement vector projected on the S^k base can be written :

$$\mathbf{q}^k = \Phi^k \eta^k \quad (7)$$

where : η^k is the generalized displacement vector of S^k.

From (7), the eigen value problem (5) confirms :

$$\left(\overline{\mathbf{K}}^k - \omega^2 \overline{\mathbf{M}}^k\right)\eta^k = \sum_l \Phi^{kT} \mathbf{B}_l^{kT} \mathbf{f}_L^k \quad (8)$$

The generalized stiffness and mass matrices are obtained by projecting the stiffness and mass matrices of the finite element model on the sub-structure base. The first vectors of the projection base are eigen vectors, so the left-top blocks of the generalized stiffness and mass matrices are diagonal (eq. 9 & 10).

$$\overline{\mathbf{K}}^k = \Phi^{kT} \mathbf{K}^k \Phi^k = \begin{bmatrix} \varphi^{kT} \mathbf{K}^k \varphi^k & \varphi^{kT} \mathbf{K}^k \psi^k \\ \psi^{kT} \mathbf{K}^k \varphi^k & \psi^{kT} \mathbf{K}^k \psi^k \end{bmatrix} = \begin{bmatrix} \overline{k}_i & 0 \\ 0 & \psi^{kT} \mathbf{K}^k \psi^k \end{bmatrix} \quad (9)$$

$$\overline{\mathbf{M}}^k = \Phi^{kT} \mathbf{M}^k \Phi^k = \begin{bmatrix} \varphi^{kT} \mathbf{M}^k \varphi^k & \varphi^{kT} \mathbf{M}^k \psi^k \\ \psi^{kT} \mathbf{M}^k \varphi^k & \psi^{kT} \mathbf{M}^k \psi^k \end{bmatrix} = \begin{bmatrix} \overline{m}_i & \varphi^{kT} \mathbf{M}^k \psi^k \\ \psi^{kT} \mathbf{M}^k \varphi^k & \psi^{kT} \mathbf{M}^k \psi^k \end{bmatrix} \quad (10)$$

The particular form of the generalized stiffness matrix is obtained by applying the definition of the constrained modes (eq. 3).

2.2 Compatibility equations

Let us consider two sub-structures S^k and S^l which have a common interface. As the movement of the structure is continuous at the interface, the interface displacements and forces are constrained by :

$$\mathbf{q}^k_{S^k \cap S^l} = \mathbf{q}^l_{S^k \cap S^l} \quad \text{and} \quad \mathbf{f}_L^k = -\mathbf{f}_L^l \quad (11)$$

The extraction matrices confirm :

$$\mathbf{q}^k_{S^k \cap S^l} = \mathbf{B}_l^k \mathbf{q}^k \quad , \quad \mathbf{q}^l_{S^k \cap S^l} = \mathbf{B}_k^l \mathbf{q}^l \quad (12)$$

From eq. 12 and eq. 7, the equation (11) can be written :

$$\mathbf{B}_l^k \Phi^k \eta^k = \mathbf{B}_k^l \Phi^l \eta^l \quad \text{and} \quad \mathbf{f}_L^k = -\mathbf{f}_L^l \quad (13)$$

2.3 Dynamic equation verified by the complete structure

The dynamic equation verified by a structure, which consists in N sub-structures, can be readily obtained from the dynamic equations of each sub-structure and the compatibility equations :

$$\left(\begin{bmatrix} \overline{\mathbf{K}}^1 & & & \\ & \ddots & & \\ & & \overline{\mathbf{K}}^k & \\ & & & \ddots \\ & & & & \overline{\mathbf{K}}^N \end{bmatrix} - \omega^2 \begin{bmatrix} \overline{\mathbf{M}}^1 & & & \\ & \ddots & & \\ & & \overline{\mathbf{M}}^k & \\ & & & \ddots \\ & & & & \overline{\mathbf{M}}^N \end{bmatrix} \right) \begin{Bmatrix} \eta^1 \\ \vdots \\ \eta^k \\ \vdots \\ \eta^N \end{Bmatrix} = \begin{Bmatrix} \sum_{l_1} \Phi^{1T} \mathbf{B}_{l_1}^{1\,T} \mathbf{f}_L^1 \\ \vdots \\ \sum_{l_k} \Phi^{kT} \mathbf{B}_{l_k}^{k\,T} \mathbf{f}_L^k \\ \vdots \\ \sum_{l_N} \Phi^{NT} \mathbf{B}_{l_N}^{N\,T} \mathbf{f}_L^N \end{Bmatrix} \quad (14)$$

$$\mathbf{B}_l^k \Phi^k \eta^k = \mathbf{B}_k^l \Phi^l \eta^l \quad \text{and} \quad \mathbf{f}_L^k = -\mathbf{f}_L^l$$

2.4 Example : structure consisting in 2 sub-structures

Let us consider a structure composed of two sub-structures, we have to solve the equation :

$$\left(\begin{bmatrix} \overline{\mathbf{K}}^1 & 0 \\ 0 & \overline{\mathbf{K}}^2 \end{bmatrix} - \omega^2 \begin{bmatrix} \overline{\mathbf{M}}^1 & 0 \\ 0 & \overline{\mathbf{M}}^2 \end{bmatrix} \right) \begin{Bmatrix} \eta^1 \\ \eta^2 \end{Bmatrix} = \begin{Bmatrix} \Phi^{1T} \mathbf{B}^{1T} \mathbf{f}_L^1 \\ \Phi^{2T} \mathbf{B}^{2T} \mathbf{f}_L^2 \end{Bmatrix} \quad (15)$$

$$\mathbf{B}^1 \Phi^1 \eta^1 = \mathbf{B}^2 \Phi^2 \eta^2 \quad \text{and} \quad \mathbf{f}_L^1 = -\mathbf{f}_L^2$$

The system can be rewritten as follows :

$$\left(\begin{bmatrix} \overline{\mathbf{K}}^1 & 0 & -\Phi^{1T} \mathbf{B}^{1T} \\ 0 & \overline{\mathbf{K}}^2 & \Phi^{2T} \mathbf{B}^{2T} \\ -\mathbf{B}^1 \Phi^1 & \mathbf{B}^2 \Phi^2 & 0 \end{bmatrix} - \omega^2 \begin{bmatrix} \overline{\mathbf{M}}^1 & 0 & 0 \\ 0 & \overline{\mathbf{M}}^2 & 0 \\ 0 & 0 & 0 \end{bmatrix} \right) \begin{Bmatrix} \eta^1 \\ \eta^2 \\ \mathbf{f}_L^1 \end{Bmatrix} = \begin{Bmatrix} 0 \\ 0 \\ 0 \end{Bmatrix} \quad (16)$$

Yet, it can be demonstrated that the stiffness matrix of this system is not always inversible. To readily inverse the stiffness matrix, we introduce the Lagrange multipliers of the system λ_1 and λ_2, which confirm :

$$\lambda_1 = -\mathbf{f}_L^1 \quad \text{and} \quad \lambda_2 = \mathbf{f}_L^2 \quad (17)$$

Then, the system to be solved has the following form :

$$\left(\begin{bmatrix} -1 & -\mathbf{B}^1 \Phi^1 & \mathbf{B}^2 \Phi^2 & 1 \\ -\Phi^{1T} \mathbf{B}^{1T} & \overline{\mathbf{K}}^1 & 0 & -\Phi^{1T} \mathbf{B}^{1T} \\ \Phi^{2T} \mathbf{B}^{2T} & 0 & \overline{\mathbf{K}}^2 & \Phi^{2T} \mathbf{B}^{2T} \\ 1 & -\mathbf{B}^1 \Phi^1 & \mathbf{B}^2 \Phi^2 & -1 \end{bmatrix} - \omega^2 \begin{bmatrix} 0 & 0 & 0 & 0 \\ 0 & \overline{\mathbf{M}}^1 & 0 & 0 \\ 0 & 0 & \overline{\mathbf{M}}^2 & 0 \\ 0 & 0 & 0 & 0 \end{bmatrix} \right) \begin{Bmatrix} \lambda_1 \\ \eta^1 \\ \eta^2 \\ \lambda_2 \end{Bmatrix} = \begin{Bmatrix} 0 \\ 0 \\ 0 \\ 0 \end{Bmatrix} \quad (18)$$

It is obvious that this system is hermitian. The size of this eigen value problem is determined by the sum of the numbers of eigen modes and static modes of the projection bases of all sub-structures. It is thus the result of a compromise between performance (cpu time) and accuracy (truncation errors).

3 Modal analysis of a turbine generator set

3.1 Introduction

AC turbogenerators are essential elements in nuclear power stations and their operation is analyzed in detail. The turbine blades at the ends of the low pressure rotors are among the elements of AC turbogenerators presenting a potential risk of vibration. To increase the power of the turbines, designers are using longer and longer blades which may be excited at low frequency by torsional stress exerted at the level of the AC generator.

3.2 Finite element model

The shaft line model which we have produced is specific to the calculation of coupled bending-torsion modes. We demonstrate that only modes with no blade phase shift can be coupled with the shaft line torsion modes. The rotor can then be modelled by means of an angular sector and conditions with satisfactory limits in terms of cyclic repetitiveness can be applied to the right and left interfaces of the sector. Such a model should enable us to calculate the response of the blades to torsional stress exerted at the level of the generator which only excited the coupled bending-torsion modes.

The main difficulties concerning modelling are due to the non-linear behaviour of the blades : untwisting of the blades through inertia, leading to large displacements and large rotations and linkage of the blades at the level of the blade fins, whose dynamic behaviour varies according to the rotation speed.

It is not particularly difficult to take into account the untwisting of the blade due to centrifugal force since the calculation of the static position of the blade at 1500 rev/min and the modal calculation are performed one after the other. The static position of a rotating structure is determined using the following exact equation :

$$\left[\mathbf{K} + \mathbf{K}_c + \mathbf{K}_g(u)\right].u = \mathbf{F}_c(u) \quad (19)$$

where: $\mathbf{K}$ is the stiffness matrix of the structure,
$\mathbf{K}_c$ is the centrifugal stiffness matrix of the structure,
$\mathbf{K}_g$ is the geometrical stiffness matrix of the structure (non-linear),
$\mathbf{F}_c$ is the centrifugal force to which the structure is subjected (non-linear),
u is the resulting displacement.

Inter-blade contact is modelled linearly, by meshing the clearance between the blade studied and the next one using classic finite elements (cf. fig 4) for which the Young modulus has been adjusted on the basis of the experimental modal results.

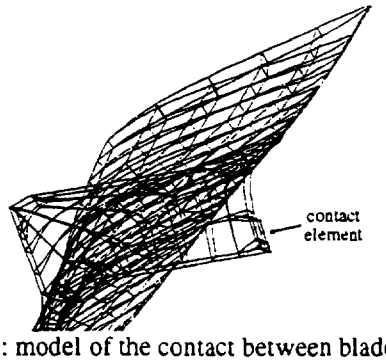

fig. 4 : model of the contact between blades

Two methods were compared for modelling the vibratory behaviour of the shaft line in order to assess the advantages of dynamic sub-structuring in terms of calculation costs :

- direct calculation,
- calculation by general dynamic sub-structuring.

For the calculation by sub-structuring, four sub-structures were defined to make the calculation : a generator, a low pressure rotor (repeated 3 times), a high pressure rotor and a blade (repeated 6 times). The final generalized system, after assembly of the sub-structures, contains 311 equations (167 sub-structure equations and 144 linkage equations).

The complete mesh of the turbine generator set, for the direct calculation, with these six blades is shown in figure 5. It contains 17,600 nodes and 3,000 meshes. The dimension of the finite element model is 65,000 degrees of freedom.

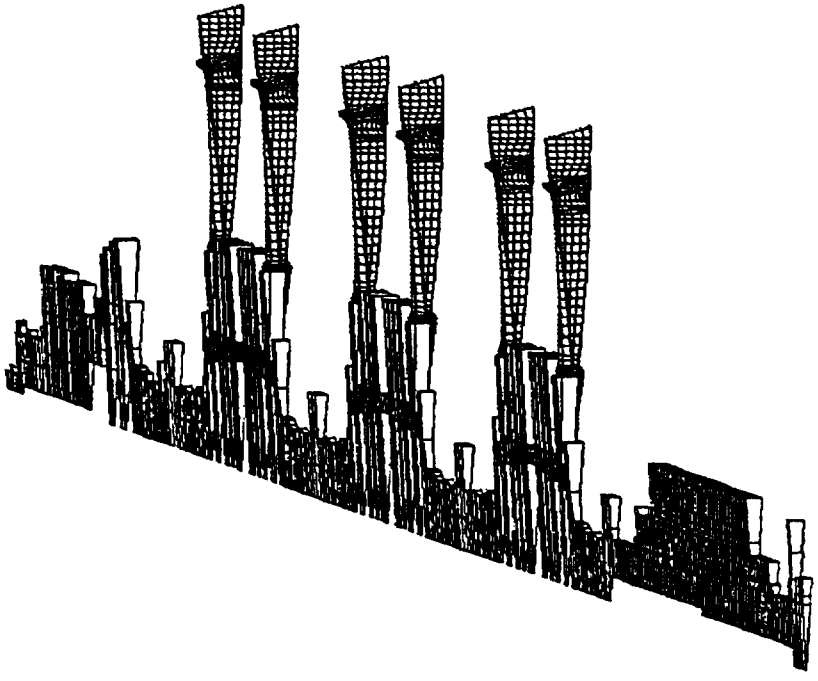

Fig. 5 : Mesh of the turbine generator set

3.3 Results

The results are presented in the table below :

Last LP rotor blading flexural eigen modes (with embedded basis)	Coupled eigen modes frequencies	
	Calculation	Difference with measurements results
Bending 1 : f	$0{,}95f$	=> 2,1 %
	$0{,}95f$	
	$0{,}95f$	
	$1{,}05f$	=> 2,0 %
	$1{,}05f$	
	$1{,}05f$	

Table 1 : results

Two calculations were performed. We first calculated the specific modes of the bladings without considering the torsion of the shaft line. This is the equivalent of embedding the blade-rotor attachment. We then calculated the specific modes while taking into account the coupling of the bending of the blades and the torsion of the shaft line.

We observe that the bending modes of the embedded end-blades are reduced into 6 coupled bending-torsion modes which are clearly organized in two subgroups of 3 modes with very similar frequencies.

Visualization of the mode shapes shows that the three modes in the first subgroup result from coupling of the bending of the blades and the torsion 1 of the low pressure rotors, while the three modes in the second subgroup result from the coupling of the bending of the blades and the torsion 0 of the LP rotors. The coupled modes differ in the value of the phase-shift between the 3 LP rotors. Figures 6 and 7 show the bending 1 - torsion 1 coupled modes and the bending 1 - torsion 0 coupled modes.

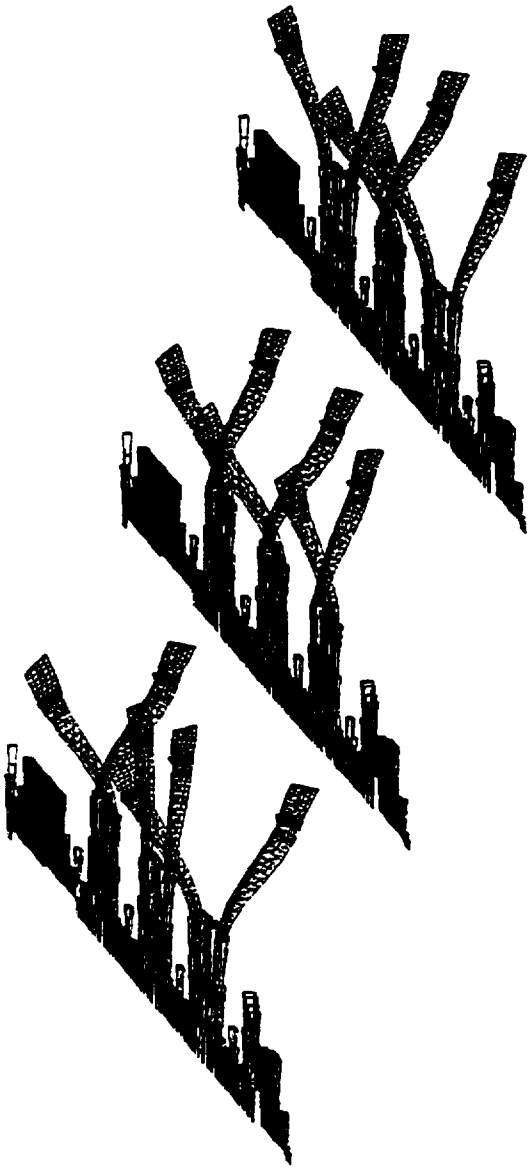

fig. 6 : coupled modes with the first shaft torsional eigen mode

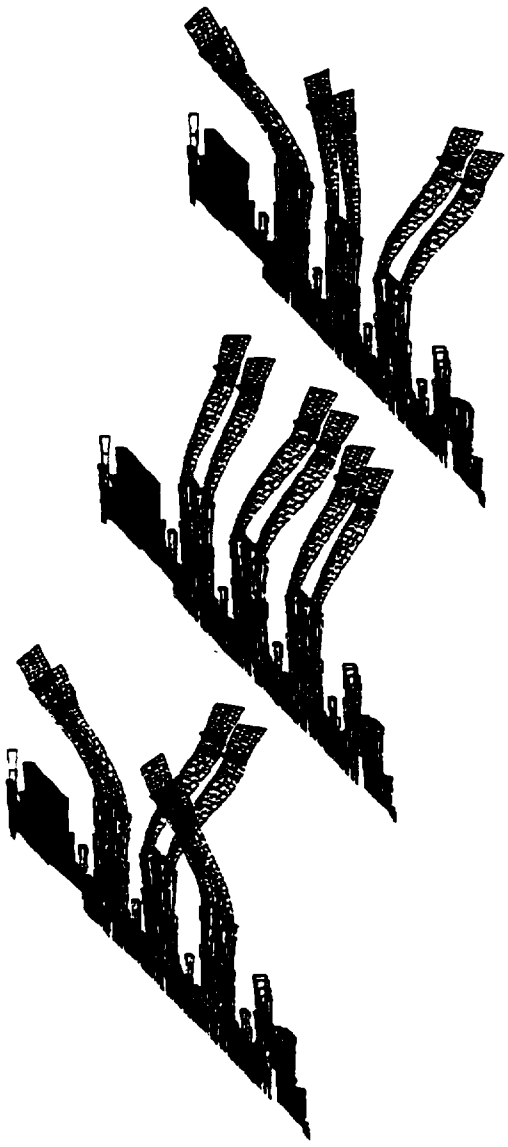

fig. 7 : coupled modes with the zero shaft torsional eigen mode

We were able to demonstrate that the results obtained by direct calculation and by general dynamic sub-structuring are identical. **The calculation time with sub-structuring, however, is much shorter (220 s compared with 1500s for direct calculation (Cray C98)).**

4 Conclusions

The eigen modes of a turbine generator set, around its equilibrium position while rotating at 1500 RPM, have been calculated with the Craig-Bampton sub-structuring method. The results were compared to measurements which have shown a coupling between the bending of the blades of the last low pressure turbine-wheels and the torsional eigen modes of the shaft (being characterized by a "frequency split" of the no nodal diameter eigen modes).

The results of the modal calculation, show good agreement with the experimental mesurements (error < 2,5%).

To have an idea of the efficiency of component mode synthesis, we decided to make the same modal analysis without using sub-structure synthesis. We find that component mode synthesis is seven times faster than direct calculation. Moreover, the difference between the two methods is very slight (error < 1%). It shows the accuracy of component mode synthesis methods.

Henceforth, it is intended to calculate the transient response of the rotor submitted to torque, caused for example by disturbances in the electrical network, and applied to the generator.

5 References

1 - EDF, *Code_Aster* (A general finite element code for thermo-mechanics developed by EDF Research and Development Division), 1993, *Internal Report* HI-75/93/034.

2 - R. R. Craig & M. C. C. Bampton, Coupling of substructures for dynamic analysis, AIAA Journal, July 1968, Vol. (6), N°7, pp. 1313-1319.

3 - R. H. Neal, A hybrid method of component mode synthesis, Computers and Structures, 1971, Vol. (1), pp. 581-601.

4 - U. Schaber, J. F. Mayer & H. Stetter, Coupled blade bending and torsional shaft vibration in turbomachinery, Proceedings of the International Gas Turbine and Aeroengine Congress and Exposition, 1993.

K. Steigleder & E. Krämer, Coupled vibrations of steam turbine blades and rotors due to torsional excitation by negative sequence currents , Proceedings of the American Power Conference, 1989.

D. J. Ewins, Vibration characteristics of bladed disc assemblies, Journal Mechanical Engineering Science, 1973, Vol. (15), N°3, pp. 165-186.